

An unprecedented trimer based on monovacant Dawson anion: $[(\alpha_2\text{-P}_2\text{W}_{17}\text{O}_{61})\text{Ln}(\text{H}_2\text{O})_4]_3^{21-}$ (Ln = La^{III}, Ce^{III} and Pr^{III})

Shaowei Zhang,^{a,b} Dongdi Zhang,^{b,c} Pengtao Ma,^{b,c} Yanfen Liang,^{b,c} Jingping Wang^{*b,c} and Jingyang Niu^{*b,d}

^a Department of Chemistry, TKL of Metal and Molecule Based Material Chemistry, Nankai University, Tianjin 300071, P. R. China

^b Polyoxometalates Chemistry Key Laboratory of Henan Province, Henan 475004, P. R. China. Fax: (+86) 378 3886876; E-mail: jyniu@henu.edu.cn, jpwang@henu.edu.cn

^c Institute of Molecular and Crystal Engineering, College of Chemistry and Chemical Engineering, Henan University, Kaifeng, Henan 475004, P. R. China

^d The State Key Laboratory of Coordination Chemistry, Nanjing University, Nanjing, Jiangsu 210093, P. R. China

Supporting Information

Fig. S1 Summary of the reported typical Ln-substituted monovacant Dawson-type POTs.

Fig. S2 Comparison of the simulated and experimental XRPD patterns: **1** (a), **2** (b) and **3** (c).

The discussion on the location of protons:

Fig. S3 Charge distribution of O atoms in the polyoxotungstate fragment $[(\alpha_2\text{-P}_2\text{W}_{17}\text{O}_{61}\text{H}_4)\text{La}(\text{H}_2\text{O})_4]^{3-}$ of **1**.

Table S1 The bond valence sum calculations of all the oxygen atoms on POM fragments in **1**.

Fig. S4 Charge distribution of O atoms in the polyoxotungstate fragment $[(\alpha_2\text{-P}_2\text{W}_{17}\text{O}_{61}\text{H}_2)\text{Ce}(\text{H}_2\text{O})_4]^{5-}$ of **2**.

Table S2 The bond valence sum calculations of all the oxygen atoms on POM fragments in **2**.

Fig. S5 The Negative mode ESI-MS of **1** in water.

Fig. S6 The TG curves of **1–3** on crystalline samples in a N₂ atmosphere in the range of 25–600 °C.

Fig. S7 IR spectra of **1–3**.

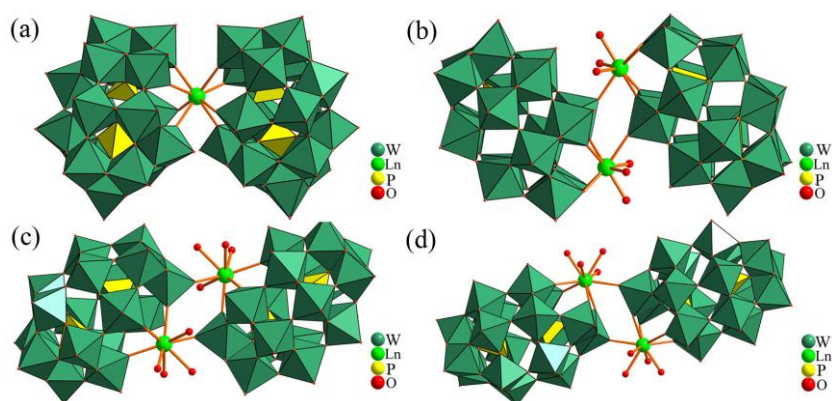


Fig. S1 Summary of the reported typical Ln-substituted monovacant Dawson-type POTs. (a) $[\text{Lu}(\alpha_1\text{-P}_2\text{W}_{17}\text{O}_{61})_2]^{17-}$; (b) $[\text{Ln}(\alpha_2\text{-P}_2\text{W}_{17}\text{O}_{61})_2]^{14-}$ ($\text{Ln} = \text{Ce}^{\text{III}}, \text{Lu}^{\text{III}}$); (c) $[\text{Ln}(\alpha_1\text{-P}_2\text{W}_{17}\text{O}_{61})_2]^{14-}$ ($\text{Ln} = \text{La}^{\text{III}}, \text{Ce}^{\text{III}}, \text{Nd}^{\text{III}}, \text{Eu}^{\text{III}}, \text{Lu}^{\text{III}}$); (d) $[\text{Ln}(\alpha_2\text{-P}_2\text{W}_{17}\text{O}_{61})_2]^{14-}$ ($\text{Ln} = \text{La}^{\text{III}}, \text{Ce}^{\text{III}}, \text{Eu}^{\text{III}}, \text{Lu}^{\text{III}}$).

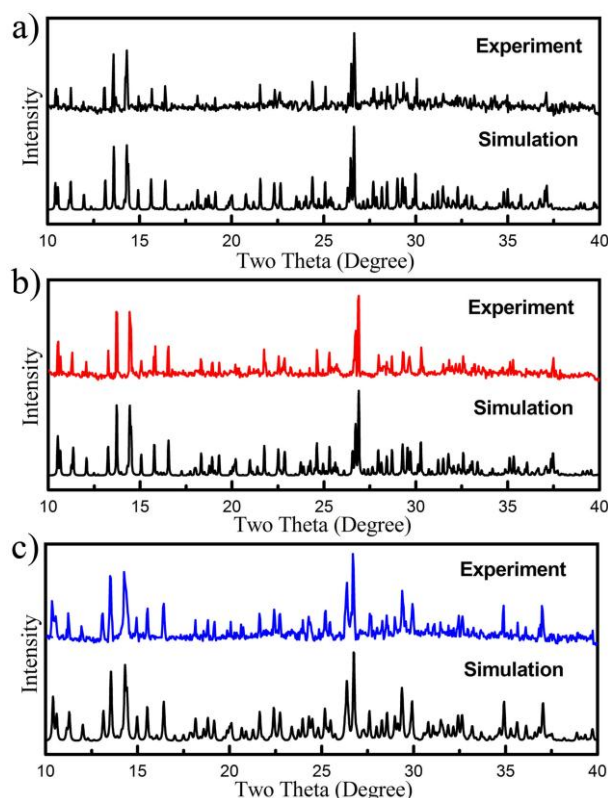


Fig. S2 Comparison of the simulated and experimental XRPD patterns: **1** (a), **2** (b) and **3** (c).

The bond-valence sum calculations suggest that all W and Ln atoms in **1–3** are in the +6 and +3 oxidation states, respectively.¹ Considering the charge balances of **1–3**, some protons need to be added. To locate the positions of these protons, the bond valence sum (Σ_s) calculations¹ of all the oxygen atoms on POM fragments are carried out (Fig. S3–S4 and Table S1–S2). The multiply protonated POM fragments in the products are reasonable based on the following considerations:^{2–10}

(i) The POM fragments $[(\alpha_2\text{-P}_2\text{W}_{17}\text{O}_{61})\text{Ln}(\text{H}_2\text{O})_4]_6^{42-}$ units in the products have high negative charges and rich basic surface oxygen atoms, which make these POM fragments easily protonated.

(ii) On the basis of the charge balance consideration and bond valence sum (Σ_s) calculations, the oxidation states of 61 O atoms in **1**, **2** and **3** can be divided into three or four groups according to the bond valence sum calculations. For **1**, there are 27 O atoms with their Σ_s in the range of $-2.08 \sim -2.01$, 11 O atoms with their Σ_s in the range of $-2.00 \sim -1.91$, and 23 O atoms with their Σ_s in the range of $-1.90 \sim -1.71$. So the four protons are likely to be delocalized on these O atoms, especially the 23 O atoms with their Σ_s in the range of $-1.90 \sim -1.71$. For **2** and **3**, the cases are the same, therefore, only **2** is taken as an

example to depict in detail. There are 30 O atoms with their Σ_s in the range of $-2.21 \sim -2.01$, 6 O atoms with their Σ_s in the range of $-2.00 \sim -1.91$, 20 O atoms with their Σ_s in the range of $-1.90 \sim -1.71$, and 5 O atoms with their Σ_s in the range of $-1.70 \sim -1.51$. So the two protons could be considered as the average bond valence sums of these O atoms, especially the 5 O atoms with their Σ_s in the range of $-1.70 \sim -1.51$.

(iii) About the synthetic conditions, the pH values of **1–3** exhibit the weak acidity. The multiple protonations of the polyoxoanion $[(\alpha_2\text{-P}_2\text{W}_{17}\text{O}_{61})\text{Ln}(\text{H}_2\text{O})_4]_6^{42-}$ with high negative charges in the products are likely under the weak acidic conditions only for the requirement of the charge balance. In the structure of **1**, there is 18 positive charges (twelve Na^+ and two $[\text{La}(\text{H}_2\text{O})_9]^{3+}$ cation), which must merge 24 protons for balancing the total 24 negative charges from itself, forming the multiply protonated POM fragment $[(\alpha_2\text{-P}_2\text{W}_{17}\text{O}_{61}\text{H}_4)\text{La}(\text{H}_2\text{O})_4]^{3-}$ in **1**. It has been confirmed by the above valence sum (Σ_s) calculations. For **2** and **3**, the cases are the same.

(iv) In generally, the multiply protons cannot be located in POM fragments by X-ray diffraction, and they are usually assigned to be delocalized on the whole POAs only for balancing the high negative charges of the POAs at different synthetic conditions, which is common in POM chemistry and has been reported in many literatures.^{2–10} From the reported results, the amount of the protons merged in the POAs with high negative charges did not absolutely depend on the acidity of the reaction system. The considerable amounts of the protons may merge in the POAs for balancing the negative charges, even in weak acidic conditions. Here, only some representative examples are shown. For example, there are 56 and 55 protons in $[\text{H}_{56}\text{P}_8\text{W}_{48}\text{Fe}_{28}\text{O}_{248}]^{28-}$ (obtained at pH = 5.2) and $[\text{H}_{55}\text{P}_8\text{W}_{49}\text{Fe}_{27}\text{O}_{248}]^{28-}$ (obtained at pH = 6.0), but they were made in the weak acidic condition, while only 4 protons in $[\text{H}_4\text{P}_2\text{W}_{12}\text{Fe}_9\text{O}_{56}(\text{OAc})_7]^{6-}$ (obtained at pH 3.7), respectively.² Other examples: $[\text{Ni}_{20}\text{P}_4\text{W}_{34}(\text{OH})_4\text{O}_{136}(\text{enMe})_8(\text{H}_2\text{O})_6]^{12-}$,³ $[\epsilon\text{-H}_4\text{PMo}^{\text{V}}_8\text{Mo}^{\text{VI}}_{36}\text{O}_{40}\{\text{La}(\text{H}_2\text{O})_4\}_4]^{5+}$,⁴ $[\text{HW}_9\text{O}_{33}\text{Ru}^{\text{II}}_2(\text{dmsO})_6]^{7-}$,⁵ $(\text{Cs}^+)_3\{[\text{18crown-6}]_3(\text{H}^+)_2\}[\text{PMo}_{12}\text{O}_{40}]$,⁶ $[\text{H}_{12}\text{V}_{13}\text{O}_{40}]^{3-}$,⁷ $[\text{H}_3\text{W}_{12}\text{O}_{40}]^{5-}$,⁸ $[\text{Sn}_4(\text{SiW}_9\text{O}_{34})_2]^{12-}$,⁹ $[(\text{H}_3\text{O})_9\{\text{PY}_2\text{W}_{10}\text{O}_{38}\}_4(\text{W}_3\text{O}_{14})]^{21-}$ and $[(\text{H}_3\text{O})_{13.5}\{\text{PEu}_2\text{W}_{10}\text{O}_{38}\}_4(\text{W}_3\text{O}_{14})]^{16.5-}$.¹⁰

- (a) N. E. Brese and M. O’Keeffe, *Acta Cryst.* 1991, **B47**, 192; (b) I. D. Brown, D. Altermatt, *Acta Cryst.* 1985, **B41**, 244.
- B. Godin, Y. G. Chen, J. Vaissermann, L. Ruhlmann, M. Verdaguer, P. Gouzerh, *Angew. Chem. Int. Ed.* 2005, **44**, 3072.
- S. T. Zheng, J. Zhang, J. M. Clemente Juan, D. Q. Yuan, G. Y. Yang, *Angew. Chem. Int. Ed.* 2009, **48**, 7176.
- P. Mialane, A. Dolbecq, L. Lisnard, A. Mallard, J. Marrot, F. Sécheresse, *Angew. Chem. Int. Ed.* 2002, **41**, 2398.
- L. H. Bi, F. Hussain, U. Kortz, M. Sadakane, M. H. Dickman, *Chem. Commun.*, 2004, 1420.
- T. Akutagawa, D. Endo, F. Kudo, S. Noro, S. Takeda, L. Cronin, T. Nakamura, *Cryst. Growth Des.* 2008, **8**, 812.
- L. Pettersson, I. Andersson, O. W. Howarth, *Inorg. Chem.* 1992, **31**, 4032.
- C. Streb, C. Ritchie, D. L. Long, P. Kögerler, L. Cronin, *Angew. Chem. Int. Ed.* 2007, **46**, 7579.
- Z. Y. Zhang, Q. P. Lin, S. T. Zheng, X. H. Bu, P. Y. Feng, *Chem. Commun.*, 2011, **47**, 3918.
- R. C. Howell, F. G. Perez, S. Jain, W. D. Horrocks, J. A. L. Rheingold, L. C. Francesconi, *Angew. Chem. Int. Ed.* 2001, **40**, 4031.

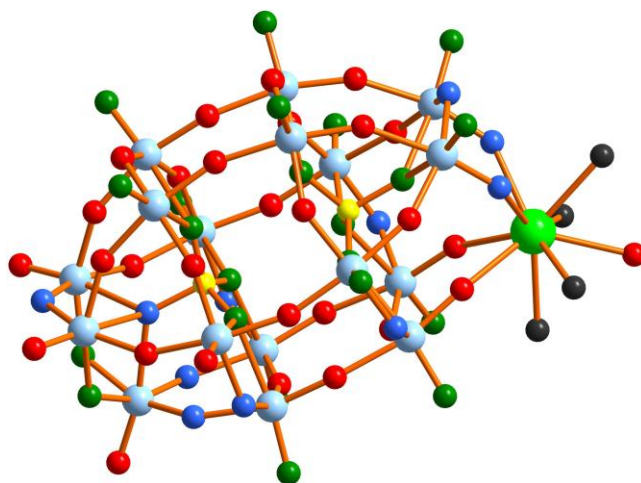





Fig. S3 Charge distribution of O atoms in the polyoxotungstate fragment $[(\alpha_2\text{-P}_2\text{W}_{17}\text{O}_{61}\text{H}_4)\text{La}(\text{H}_2\text{O})_4]^{3-}$ of **1**. Oxygen atoms with different bond valence sums are represented by different colors. H atoms, Na^+ , lattice water molecules and the discrete $[\text{La}(\text{H}_2\text{O})_9]^{3+}$ cation are omitted for clarity.

Table S1. The bond valence sum calculations of all the oxygen atoms on POM fragments in **1**.

Oxygen	Band valence sum range	Number	Oxygen	Band valence sum range	Number
	-2.08 ~ -2.01	27		-1.90 ~ -1.71	23
	-2.00 ~ -1.91	11			

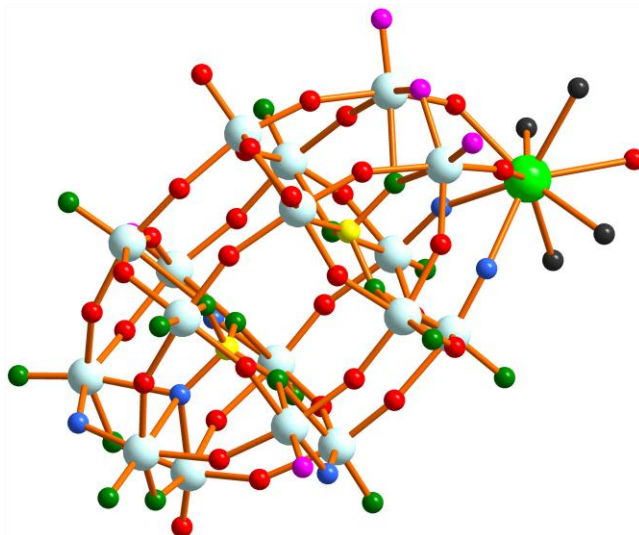






Fig. S4 Charge distribution of O atoms in the polyoxotungstate fragment $[(\alpha_2\text{-P}_2\text{W}_{17}\text{O}_{61}\text{H}_2)\text{Ce}(\text{H}_2\text{O})_4]^{5-}$ of **2**. Oxygen atoms with different bond valence sums are represented by different colors. H atoms, Na^+ , lattice water molecules and the discrete $[\text{Ce}(\text{H}_2\text{O})_8]^{3+}$ cation are omitted for clarity.

Table S2. The bond valence sum calculations of all the oxygen atoms on POM fragments in **2**.

Oxygen	Band valence sum range	Number	Oxygen	Band valence sum range	Number
	-2.21 ~ -2.01	30		-1.90 ~ -1.71	20
	-2.00 ~ -1.91	6		-1.70 ~ -1.51	5

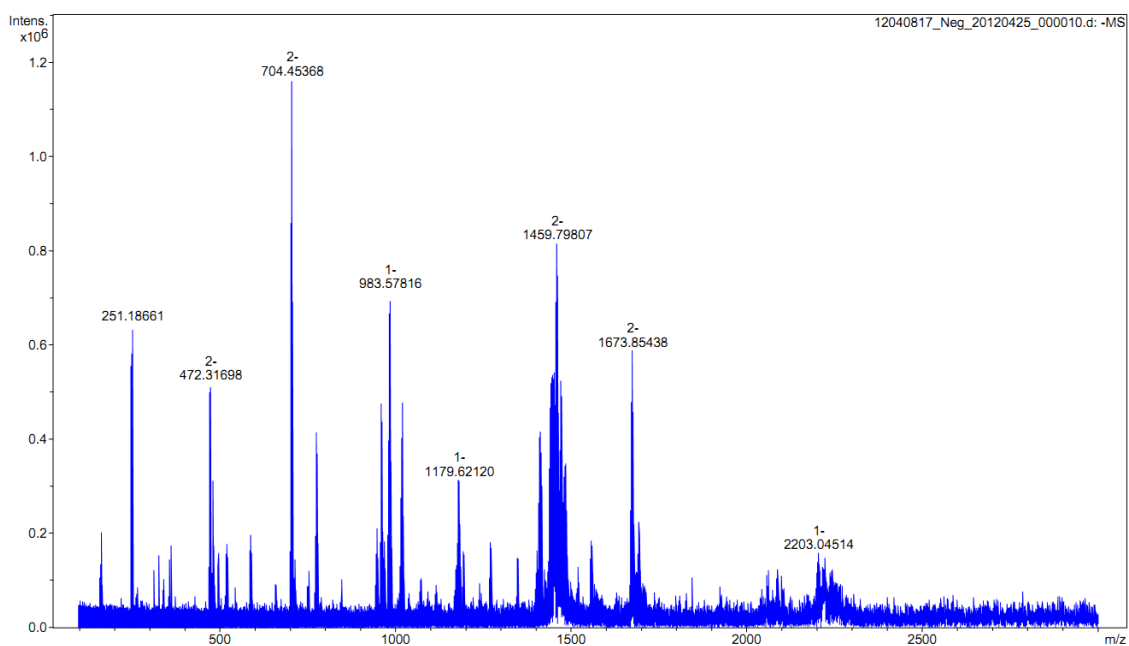


Fig. S5 The Negative mode ESI-MS of **1** in water.

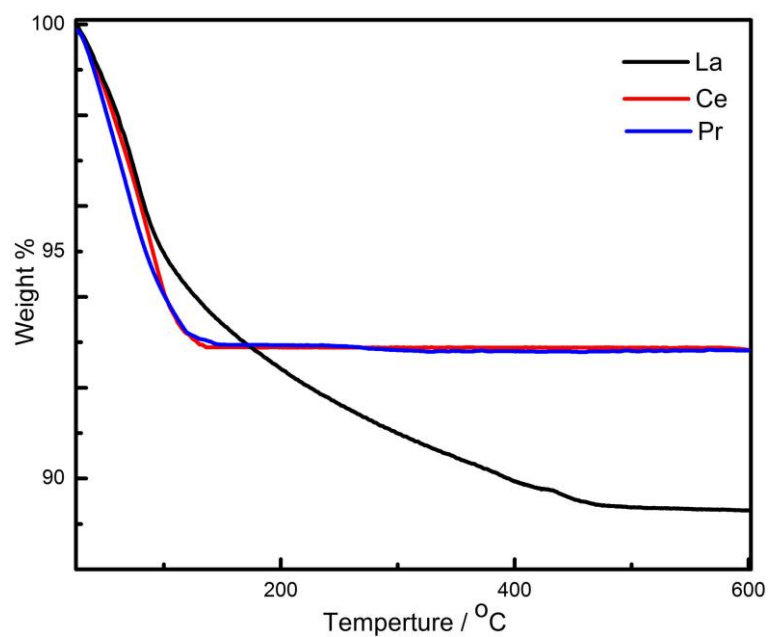


Fig. S6 The TG curves of 1–3 on crystalline samples in a N₂ atmosphere in the range of 25–600 °C.

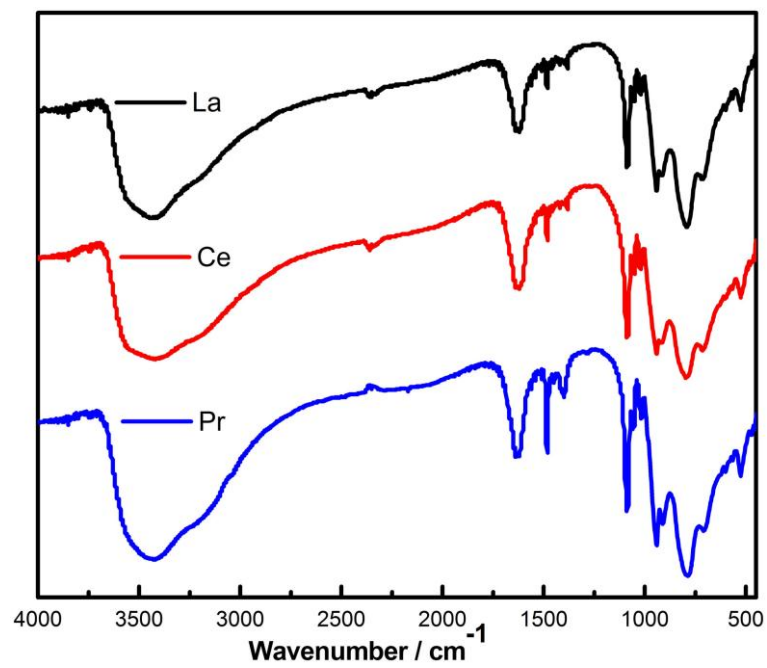


Fig. S7 IR spectra of 1–3.